

---

# Princeton Plasma Physics Laboratory

---

PPPL-

PPPL-



Prepared for the U.S. Department of Energy under Contract DE-AC02-09CH11466.

# Princeton Plasma Physics Laboratory

## Report Disclaimers

---

### Full Legal Disclaimer

This report was prepared as an account of work sponsored by an agency of the United States Government. Neither the United States Government nor any agency thereof, nor any of their employees, nor any of their contractors, subcontractors or their employees, makes any warranty, express or implied, or assumes any legal liability or responsibility for the accuracy, completeness, or any third party's use or the results of such use of any information, apparatus, product, or process disclosed, or represents that its use would not infringe privately owned rights. Reference herein to any specific commercial product, process, or service by trade name, trademark, manufacturer, or otherwise, does not necessarily constitute or imply its endorsement, recommendation, or favoring by the United States Government or any agency thereof or its contractors or subcontractors. The views and opinions of authors expressed herein do not necessarily state or reflect those of the United States Government or any agency thereof.

### Trademark Disclaimer

Reference herein to any specific commercial product, process, or service by trade name, trademark, manufacturer, or otherwise, does not necessarily constitute or imply its endorsement, recommendation, or favoring by the United States Government or any agency thereof or its contractors or subcontractors.

---

## PPPL Report Availability

### Princeton Plasma Physics Laboratory:

<http://www.pppl.gov/techreports.cfm>

### Office of Scientific and Technical Information (OSTI):

<http://www.osti.gov/bridge>

---

### Related Links:

[U.S. Department of Energy](#)

[Office of Scientific and Technical Information](#)

[Fusion Links](#)

# Numerical calculations demonstrating complete stabilization of the ideal magnetohydrodynamic resistive wall mode by longitudinal flow

S.P. Smith\* and S.C. Jardin  
*Princeton University Plasma Physics Laboratory*

J.P. Freidberg  
*Massachusetts Institute of Technology*

L. Guazzotto  
*U. of Rochester*  
 (Dated: April 28, 2009)

The cylindrical ideal magnetohydrodynamic (MHD) stability problem, including flow and a resistive wall, is cast in the standard mathematical form,  $\omega \mathcal{A} \cdot \mathbf{x} = \mathcal{B} \cdot \mathbf{x}$ , without discretizing the vacuum regions surrounding the plasma. This is accomplished by means of a finite element expansion for the plasma perturbations, by coupling the plasma surface perturbations to the resistive wall using a Green's function approach, and by expanding the unknown vector,  $\mathbf{x}$ , to include the perturbed current in the resistive wall as an additional degree of freedom. The ideal MHD resistive wall mode (RWM) can be stabilized when the plasma has a uniform equilibrium flow such that the RWM frequency resonates with the plasma's Doppler-shifted sound continuum modes. The resonance induces a singularity in the parallel component of the plasma perturbations, which must be adequately resolved. Complete stabilization within the ideal MHD model (i.e. without parallel damping being added) is achieved as the grid spacing in the region of the resonance is extrapolated to 0 step size.

PACS numbers: 52.35.-g, 52.35.Bj, 52.35.Dm

One of the main goals of the tokamak plasma community is to establish the physics principles which are the fundamental building blocks for realizing a nuclear fusion power plant based on a magnetic confinement configuration. Self sustained fusion reactions require high pressure plasmas, which are subject to instabilities. One such instability is the resistive wall mode (RWM) - an external kink mode that would be stable if the resistivity of a nearby wall were zero. A proven method to stabilize the RWM is for the plasma to have equilibrium flow [1]. This method has also been explored theoretically [2] and numerically [3, 4].

In this Letter, we demonstrate a new approach [5] for modeling the plasma-wall system in the simplified geometry of a cylindrical plasma, and apply the resulting code to find a window of wall locations where the RWM is stabilized by flow. In contrast to previous studies [3, 4], this complete stabilization is obtained without adding parallel damping to the ideal magnetohydrodynamic (MHD) model. Our approach couples the plasma, which has an equilibrium flow, to the resistive wall by using a Green's function, so that the vacuum region is not discretized. The final form of the stability problem is in the standard mathematical form  $\omega \mathcal{A} \cdot \mathbf{x} = \mathcal{B} \cdot \mathbf{x}$ , such that standard eigenvalue solvers can be used. We present numerical results showing that the RWM is stabilized by uniform equilibrium plasma flow for a range of wall positions. This stabilization occurs in the limit of infinite resolution around the RWM-sound resonant surface.

The plasma has an equilibrium state characterized by

the usual ideal MHD quantities  $\rho$ ,  $p$ ,  $\mathbf{B}$ ,  $\mathbf{J}$ , and  $\gamma$ , as well as an equilibrium flow  $\mathbf{V}$ . In a circular cylindrical geometry  $(r, \theta, z)$  the MHD equilibrium equation is

$$\mu_0 p' + (B^2)' / 2 + B_\theta^2 / r = \mu_0 r \rho \Omega^2,$$

where  $\{\}' \equiv \frac{d}{dr} \{\}$ ,  $\Omega \equiv \mathbf{V} \cdot \hat{\boldsymbol{\theta}} / r$ , and all equilibrium quantities are only a function of  $r$ . The plasma exists in the region  $0 < r < a$ .

Perturbations about the equilibrium obey the equations

$$\omega \rho \boldsymbol{\xi} = \rho \mathbf{u} - i \rho \mathbf{V} \cdot \nabla \boldsymbol{\xi} \quad (1)$$

$$\omega \rho \mathbf{u} = -\tilde{\mathbf{J}} \times \mathbf{B} - \mathbf{J} \times \tilde{\mathbf{B}} + \nabla \tilde{p} - \nabla \cdot [\boldsymbol{\xi} (\rho \mathbf{V} \cdot \nabla \mathbf{V})] - i \rho \mathbf{V} \cdot \nabla \mathbf{u}. \quad (2)$$

Here  $\tilde{\mathbf{B}} = \nabla \times (\boldsymbol{\xi} \times \mathbf{B})$ ,  $\tilde{\mathbf{J}} = \nabla \times \tilde{\mathbf{B}} / \mu_0$ ,  $\tilde{p} = -\boldsymbol{\xi} \cdot \nabla p - \gamma p \nabla \cdot \boldsymbol{\xi}$ ,  $\boldsymbol{\xi}$  is the usual Lagrangian displacement,  $\mathbf{u}$  has been introduced so that the eigenvalue,  $\omega$ , only appears linearly, and the components of  $\boldsymbol{\xi}$  and  $\mathbf{u}$  vary as  $e^{i(m\theta + kz - \omega t)}$ . The dependence on  $\omega$  is such that a mode with  $\text{Im}(\omega) (\equiv \Gamma) > 0$  is an instability.

An appropriate set of projections, based on Chance et al. [6], decouples the parallel displacements from the perpendicular displacements and allows for  $\nabla \cdot \boldsymbol{\xi}_\perp = 0$  or  $\nabla \cdot \boldsymbol{\xi} = 0$ , if an appropriate finite element decomposition is also used. The projections are

$$\begin{aligned} \xi_r &= (\xi_1 + m \xi_2) / r & \xi_\theta &= i \left( \frac{d \xi_2}{dr} + B_\theta \xi_3 \right) \\ \xi_z &= i \left( -\frac{B_\theta}{B_z} \frac{d \xi_2}{dr} + \xi_3 B_z \right) \end{aligned}$$

or

$$\boldsymbol{\xi} = \frac{\xi_1}{r} \hat{\mathbf{r}} + i \frac{\mathbf{B}}{B_z} \times \tilde{\nabla}_\perp \xi_2 + i \xi_3 \mathbf{B},$$

with similar projections for  $\mathbf{u}$ , where  $\tilde{\nabla}_\perp \equiv \frac{d}{dr} \hat{\mathbf{r}} + \frac{1}{r} \frac{d}{d\theta} \hat{\boldsymbol{\theta}}$ . Each of the unknown eigenfunctions,  $\xi_1(r) \dots u_3(r)$ , is expanded as a sum of  $N$  expansion functions,

$$\begin{aligned} \xi_1(r) &= \sum \xi_{1j} \phi_{1j}(r), & \xi_2(r) &= \sum \xi_{2j} \phi_{2j}(r), \\ \xi_3(r) &= \sum \xi_{3j} \phi_{3j}(r), & \text{etc.} \end{aligned}$$

The finite elements used are defined by

$$\phi_{1j} = \begin{cases} \frac{\int_{r_{j-1}}^r B_\theta r / B_z dr}{\int_{r_{j-1}}^{r_j} B_\theta r / B_z dr} & \text{if } r_{j-1} < r < r_j \\ \frac{\int_r^{r_{j+1}} B_\theta r / B_z dr}{\int_{r_j}^{r_{j+1}} B_\theta r / B_z dr} & \text{if } r_j < r < r_{j+1} \\ 0 & \text{otherwise} \end{cases},$$

$$\phi_{2j} = \begin{cases} \frac{r - r_{j-1}}{r_j - r_{j-1}} & \text{if } r_{j-1} < r < r_j \\ \frac{r_{j+1} - r}{r_{j+1} - r_j} & \text{if } r_j < r < r_{j+1} \\ 0 & \text{otherwise} \end{cases},$$

$$\phi_{3j} = \begin{cases} 1 & \text{if } r_{j-1} < r < r_j \\ 0 & \text{otherwise} \end{cases}.$$

The particular form of  $\phi_{1j}$  stems from the need to allow

$$\nabla \cdot \boldsymbol{\xi}_\perp = \frac{1}{r} \frac{d\xi_1}{dr} + k \frac{B_\theta}{B_z} \frac{d\xi_2}{dr} = 0,$$

to machine precision, to avoid spectral pollution [6].

The traditional Galerkin approach is to multiply some projection of the starting equations [in our case Eqs. (1) and (2)] by a test function then integrate over all space. The necessary projections, test functions, and integrals are

$$\int_0^a r dr \frac{\phi_{1i}}{r} e^{-i(m\theta + kz - \omega t)} \hat{\mathbf{r}}, \quad (3)$$

$$\begin{aligned} & \left\{ -i \int_0^a r dr \phi_{2i} e^{-i(m\theta + kz - \omega t)} \tilde{\nabla}_\perp \cdot \frac{1}{B_z} \mathbf{B} \times \right\}, \\ & + \left\{ i \phi_{2i} e^{-i(m\theta + kz - \omega t)} r \hat{\mathbf{r}} \cdot \frac{1}{B_z} \mathbf{B} \times \right\}_{r=a}, \end{aligned} \quad (4)$$

and

$$-i \int_0^a r dr \phi_{3i} e^{-i(m\theta + kz - \omega t)} \mathbf{B}, \quad (5)$$

where

$$\tilde{\nabla}_\perp \cdot = \frac{1}{r} \frac{d}{dr} \left( r \hat{\mathbf{r}} \cdot \right) + \frac{im}{r} \hat{\boldsymbol{\theta}} \cdot \dots$$

Note that the surface projection in Eq. (4) is needed as a boundary condition for the differential operator.

The method for coupling the plasma surface perturbations to the resistive wall by means of a Green's function extends the method in Smith and Jardin [7] to a plasma with flow. The thin resistive wall located at  $r = b$ , has a conductivity,  $\sigma$ , and a thickness,  $d (\ll b)$ , such that  $\tau_w = \mu_0 \sigma db$  is the characteristic diffusion time of the perturbed magnetic field through the wall. The perturbed current in the wall is  $\mathbf{j}_{rw} = \nabla [j_s e^{i(m\theta + kz - \omega t)}] \times \hat{\mathbf{r}}$ , where  $j_s$  is a new unknown constant. The jump condition on the perturbed magnetic field across the wall can then be expressed as

$$\frac{\omega \tau_w b \dot{K}_b}{(m^2 + k^2 b^2) \dot{K}_a} \left[ \xi_1(a) \alpha - \mu_0 j_s i k \frac{\dot{I}_a \dot{K}_b - \dot{I}_b \dot{K}_a}{\dot{I}_b \dot{K}_b - \dot{I}_a \dot{K}_a} \right] = -\mu_0 j_s. \quad (6)$$

The vacuum perturbed pressure at the plasma surface,

$$\left[ \mathbf{B} \cdot \tilde{\mathbf{B}} / \mu_0 \right]_{vac} = j_s i \alpha \frac{\dot{I}_a \dot{K}_a - \dot{I}_a K_a \dot{K}_b}{\dot{I}_b \dot{K}_b - \dot{I}_b K_b \dot{K}_a} - \xi_1(a) \alpha^2 \frac{K_a}{\mu_0 k \dot{K}_a},$$

replaces the plasma perturbed pressure at the plasma surface through the jump condition

$$\left[ \tilde{p} + \mathbf{B} \cdot \tilde{\mathbf{B}} / \mu_0 \right]_{plasma} = \left[ \mathbf{B} \cdot \tilde{\mathbf{B}} / \mu_0 \right]_{vac}.$$

The notation used is  $\alpha \equiv m B_\theta(a) / a + k B_z(a)$ ,  $K_a \equiv K_m(ka)$ ,  $\dot{K}_a \equiv \left[ \frac{d}{d(kr)} K_m(kr) \right]_{r=a}$ , etc, where  $K_m$  and  $I_m$  are modified Bessel functions.

We now have  $6N + 1$  equations [ $3N$  operators of Eqs. (3)-(5)  $\times$  2 equations of Eqs. (1) and (2) + 1 equation from Eq. (6)] and  $6N + 1$  unknowns,  $\mathbf{x} = (\xi_{1j}, \xi_{2j}, \xi_{3j}, u_{1j}, u_{2j}, u_{3j}, j_s)$ , whose relationship can be expressed in the standard mathematical form,  $\omega \mathcal{A} \cdot \mathbf{x} = \mathcal{B} \cdot \mathbf{x}$ . Once in this form, the generalized eigenvalue equation can be solved by any standard matrix eigensolver; we have used the LAPACK routine ZGGEVX [8].

We examine the stability of an equilibrium having the form

$$\begin{aligned} B_z &= [B_{z0}^2 a^2 + 2(B_{\theta0}^2 - p_0)(a^2 - r^2)]^{1/2} / a, & V_z &= V_{z0} \\ \rho &= \rho_0, & p &= p_0 (1 - r^2/a^2) / \mu_0, & B_\theta &= B_{\theta0} r / a. \end{aligned} \quad (7)$$

The effect on the RWM of adding uniform axial flow can be seen in Fig. 1, which shows the sound modes and RWMs of the stability spectra in the complex plane for various flow rates. As expected, the main effect of the flow is to Doppler shift the normal sound frequencies by the amount  $kV_{z0}$ . For clarity, the damped RWMs are marked as label 1 in Fig. 1a and the RWM as label 2. Several interesting features need to be pointed out in Fig. 1. First, the damped RWM at label 1 occurs at the same frequency,  $\omega_I$ , as would the stabilized kink mode for an ideal wall at the same location [7]. Next, the RWM is

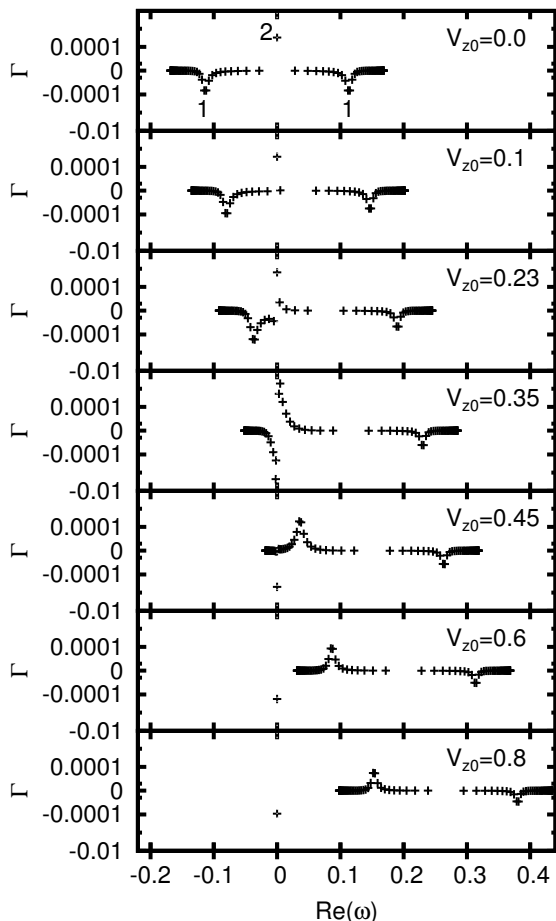


FIG. 1: Sound and RWM region of the ideal MHD stability spectrum in the complex  $\omega$  plane for a system [see Eq. (7)] specified by  $a = 1$ ,  $p_0 = 0.7981111245\mu_0$ ,  $\rho_0 = 1$ ,  $B_{z0} = 10$ ,  $B_{\theta0} = 1.6307189542$ ,  $b = 1.625$ ,  $\tau_w = 4 \times 10^5$ ,  $m = 3$  and  $k = 1/3$  for various flow rates,  $V_{z0}$ , using  $N = 40$  finite elements in the plasma. The inverse hyperbolic sine scale for  $\Gamma$  behaves like a logarithmic scale far from 0 and a linear scale close to zero. The labels are described in the text.

not damped by the sound modes until the Doppler-shift is sufficient to cause a resonance of the RWM with the sound modes located around  $\omega_I$  (i.e.  $kV_{z0} > \omega_I$ ). Finally, the RWM resonates at the Doppler shifted ideal wall frequency for higher flow rates ( $\omega_{\text{RWM}} = \omega_I + kV_{z0}$ ). From these three observations, one could determine the absolute minimum amount of flow needed to start damping the RWM, the resonant frequency of the RWM, and the location in the plasma of the resonance, all from the stationary plasma spectrum for a given wall location.

For  $V_{z0} = 0.6$  the Doppler shift is sufficient for the RWM to resonate with any of the sound modes, so this value will be chosen for the remainder of the results. It is worthwhile to examine the nature of the RWM as we increase the number of finite elements used. In Fig. 2, we see that the RWM growth rate decreases as the number of elements increases. By looking at the  $\xi_3 (= \xi_{\parallel})$  eigen-

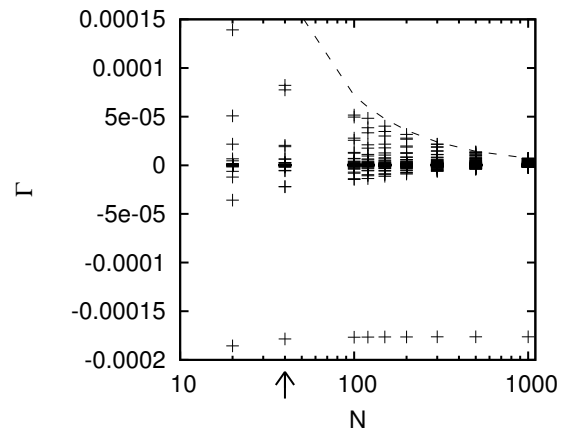


FIG. 2: Convergence of the growth and damping rates with the number of uniformly spaced finite elements used for the system specified in Fig. 1 and  $V_{z0} = 0.6$ . The dotted line is proportional to  $1/N$ . Note that the points indicated by the arrow are plotted in Fig. 1 ( $V_{z0} = 0.6$ ).

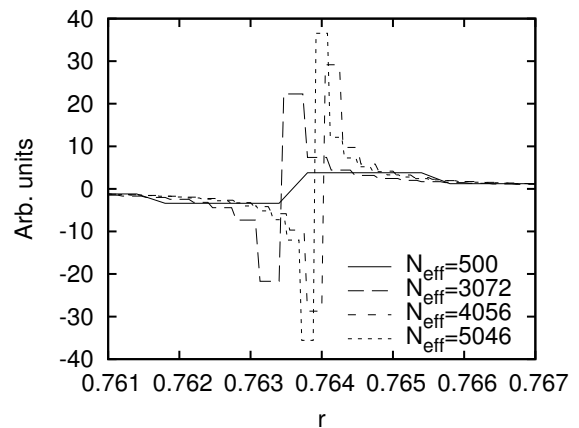


FIG. 3: The real part of the  $\xi_3$  eigenfunction of the RWM for a grid packed around the resonant surface, where  $N_{\text{eff}}$  would be the number of equally spaced grid points spread across the whole plasma. The displacement is normalized such that  $\xi_r|_{r=a} = 1 + 0i$ . Parameters are given in Fig. 1, with  $V_{z0} = 0.6$ .

functions in Fig. 3 for a grid that is localized around the resonant surface, we see that there is a singular structure which is not resolved even by a grid with an equivalent of  $N \sim 5000$  points. Fig. 4 indicates that the amplitude of the eigenfunctions (+) is approaching  $\infty$  as the grid spacing around the singular location,  $h_{\text{min}}$ , vanishes. Because the true singular nature of the eigenfunction is only approached as  $h_{\text{min}} \rightarrow 0$ , then it can be expected that the growth rate will have a similar behavior. Thus, although the RWM is not completely stabilized for any finite grid spacing, the growth rate ( $\times$  in Fig. 4) is extrapolated to a slightly negative (damped) value for  $h_{\text{min}} \rightarrow 0$ .

Looking at the growth rate extrapolated to  $h_{\text{min}} \rightarrow 0$  for various wall locations reveals that there is a window

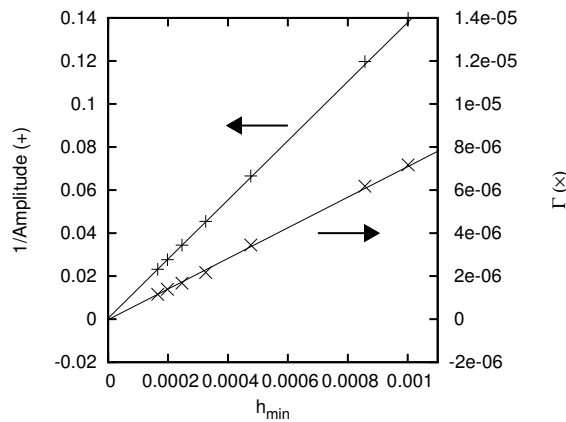


FIG. 4: The inverse of the amplitude (+) of the real part of the  $\xi_3$  eigenfunction (see Fig. 3) converges to zero as the grid spacing,  $h_{min}$ , around the singular location vanishes ( $h_{min} \rightarrow 0$ ). The growth rate of the RWM (x) converges to a slightly damped value for  $h_{min} \rightarrow 0$ . The lines are extrapolations from the two smallest  $h_{min}$ .

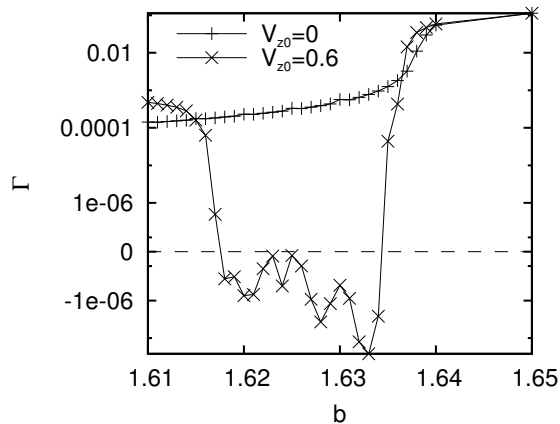


FIG. 5: The RWM extrapolated growth rate for various wall locations,  $b$ , and flow rates,  $V_{z0}$  for the system specified in Fig. 1. The inverse hyperbolic sine scale is used again for  $\Gamma$ .

of wall locations for completely stabilizing the RWM with flow (see Fig. 5). A similar analytic limit had been solved for previously [2], but has not been shown numerically without adding explicit damping terms to Eq. (2). The level to which the RWM is damped in Fig. 5 is less than the level of damping given by the analytic limit of Ref. 2; this difference may be due to the difference between the perturbative approach taken to arrive at the analytic limit (where the eigenfunctions from the RWM without flow are used to calculate the growth rate), and the self-consistent approach taken here.

The extrapolation to zero step size flow stabilization has been shown explicitly for  $V_{z0} = 0.6$ . This stabilization also occurs, though it is not shown here, for the same range of wall locations for  $V_{z0} = 0.8$  and for a narrower range of wall locations for  $V_{z0} = 0.45$ .

To summarize, we have demonstrated numerically that the ideal MHD RWM can be stabilized by uniform flow without additional dissipation. However, great care must be taken to represent the plasma displacements with a field-aligned projection and appropriate finite elements to avoid spectral pollution. Furthermore, the resonance between the sound modes and the RWM induces a singularity in the field aligned displacement, which can only be adequately resolved in the limit  $h_{min} \rightarrow 0$ . Future investigations will focus on the effects of flow shear localized around the resonant surface. Finally, some insight can be gained by looking at the entire spectrum of the plasma-wall system, which is made possible by casting the entire stability problem as a standard eigenvalue problem.

The work of S. P. Smith was partly performed under appointment to the Fusion Energy Sciences Fellowship Program administered by Oak Ridge Institute for Science and Education under a contract between the United States Department of Energy (U.S. DOE) and the Oak Ridge Associated Universities. This work was also supported by U.S. DOE Contract No. DE-AC02-76CH0307.

\* Electronic address: [spsmith@pppl.gov](mailto:spsmith@pppl.gov);  
URL: [www.pppl.gov/~spsmith](http://www.pppl.gov/~spsmith)

- [1] E. J. Strait, T. S. Taylor, A. D. Turnbull, J. R. Ferron, L. L. Lao, B. Rice, O. Sauter, S. J. Thompson, and D. Wróblewski, Phys. Rev. Lett. **74**, 2483 (1995).
- [2] R. Betti and J. P. Freidberg, Phys. Rev. Lett. **74**, 2949 (1995).
- [3] A. Bondeson and D. J. Ward, Phys. Rev. Lett. **72**, 2709 (1994).
- [4] M. S. Chu, J. M. Greene, T. H. Jensen, R. L. Miller, A. Bondeson, R. W. Johnson, and M. E. Mauel, Physics of Plasmas **2**, 2236 (1995).
- [5] L. Guazzotto, J. P. Freidberg, and R. Betti, Physics of Plasmas **15**, 072503 (2008).
- [6] M. S. Chance, J. M. Greene, R. C. Grimm, and J. L. Johnson, Nuclear Fusion **17**, 65 (1977).
- [7] S. P. Smith and S. C. Jardin, Physics of Plasmas **15**, 080701 (2008).
- [8] E. Anderson, Z. Bai, C. Bischof, S. Blackford, J. Demmel, J. Dongarra, J. Du Croz, A. Greenbaum, S. Hammarling, A. McKenney, et al., *LAPACK Users' Guide* (Society for Industrial and Applied Mathematics, Philadelphia, PA, 1999), 3rd ed., ISBN 0-89871-447-8 (paperback).



The Princeton Plasma Physics Laboratory is operated  
by Princeton University under contract  
with the U.S. Department of Energy.

Information Services  
Princeton Plasma Physics Laboratory  
P.O. Box 451  
Princeton, NJ 08543

Phone: 609-243-2750  
Fax: 609-243-2751  
e-mail: [pppl\\_info@pppl.gov](mailto:pppl_info@pppl.gov)  
Internet Address: <http://www.pppl.gov>